Jour. Indian Association of Sedimentologists, Vol. 34, Nos. 1 & 2. (2017), pp. 39-57

Geochemical Characteristics of Proterozoic Carbonate Lithofacies of Indravati Basin, Chhatisgarh, Central India: Implication of Depositional and Diagenetic History

Rajeeva Guhey[1] and MahenderKotha[2]
[1]Department of Geology, Govt. N. P.G. College of Science, Raipur, Chhattisgarh
[2] Department of Earth Science, Goa University, Goa
Email: guheygeol@gmail.com

Abstract: The intra-cratonic Proterozoic Indravati Basin, Central India, located on the south eastern margin of the Bastar craton is represented by a Lower clastic and the Upper carbonate succession. The upper carbonate succession is represented by two formations namely the Kanger Limestone Formation (the non-stromatolitic platform) which is overlain by the Jagdalpur Formation (the stromatolitic carbonate platform). Present work provides new field and petrological observations and high precision selected trace and REE data from carbonates in order to interpret the depositional conditions of these rocks. The two carbonate lithofacies (A & C) identified on the basis of their field occurrences, distinctive petrographic and geochemical characters. The lithofacies A is a bedded micritic limestone, devoid of any allochems and the lithofacies-C is a dolomitized, stromatolite bearing limestone. Detailed petrographic observation and geochemical characters suggest an early to late diagenesis involving the processes of compaction, dissolution, cementation, recrystallization and replacement. The trace element geochemistry from number of samples shows that they are characteristic of shallow water deposits. Although a similar pattern of REE abundances resembling to that of modern seawater has been observed for all the carbonate samples with depleted LREE, the greatly enriched HREE and negative Eu anomaly, the positive Ce anomaly deviates from the modern seawater patterns. All the carbonate samples display a distinctive negative Eu anomaly. The La N/Yb N ratio of 3.64 for Lithofacies A and 3.31 for Lithofacies C samples indicates a relatively moderate degree of REE fractionation. The trace and rare earth geochemistry together with sedimentological data strongly support deposition of Kanger (lower bedded limestone) in subtidal condition and Jagdalpur (upper stromatolitic) carbonate Formation in shallow marine intertidal-supratidal condition. The change in depositional and diagenetic conditions is further substantiated by factor analysis of the geochemical data which clearly differentiates the two carbonate lithofacies.

Keywords: REE, Proterozoic carbonates, Geochemistry, Indravati, palaeoenvironment, Diagenesis.

INTRODUCTION

The Indravati Basin, covering an area of 9000 km^2 in Kanker Baster and Dantewara districts of Chhattisgarh and Koraput of Orissa (Fig.1), representing good outcrops of the Proterozoic Indravati Group of sediments, is one of the important Purana basins adjacent to Proterozoic Chhattisgarh Basin, and has been studied over last few decades. However, it is particularly in the last few years their have been a surge of research, in part on age determination and depositional environments and the age of the both Chhattisgarh and Indravati basins. Mainkar et al.(2004) proposed La-ICPMS, U-Pb age 620 $\pm$ 30 Ma on the basis of Tokapal and Bhejripadar kimberlite pyroclastics within Kanger Formation. Mukherjee et al., 2012 did U-Pb isotopic analyses (LA MC-ICPMS) of the zircons from the Birsaguda tuff, within the Jagdalpur Formation point to closure of the basin at 1001 ± 7 Ma.

Although, the geochemical nature of sediment has been better utilized in the interpretation of the depositional setting and diagenesis in Phanerozoic sequences leading generation of large data bases, the geochemical data on even well-defined sedimentary suits of Precambrian, Proterozoic sequences are very limited. The present global correlation based on carbon isotope profile curve and trace element geochemistry for origin and chronostratigraphic? implications on Indravati Basin is still lacking. The present study reports geological, petrographic and geochemical (selected Trace and REE+Y) data in order to test firstly, the compatibility of a marine precipitate origin for the carbonates and secondly compatibility with microbial involvement in carbonate precipitation and stromatolite construction.

Trace metal concentrations recorded in carbonate sediments are commonly used for palaeoenvironmental reconstruction through examination of redox-sensitive

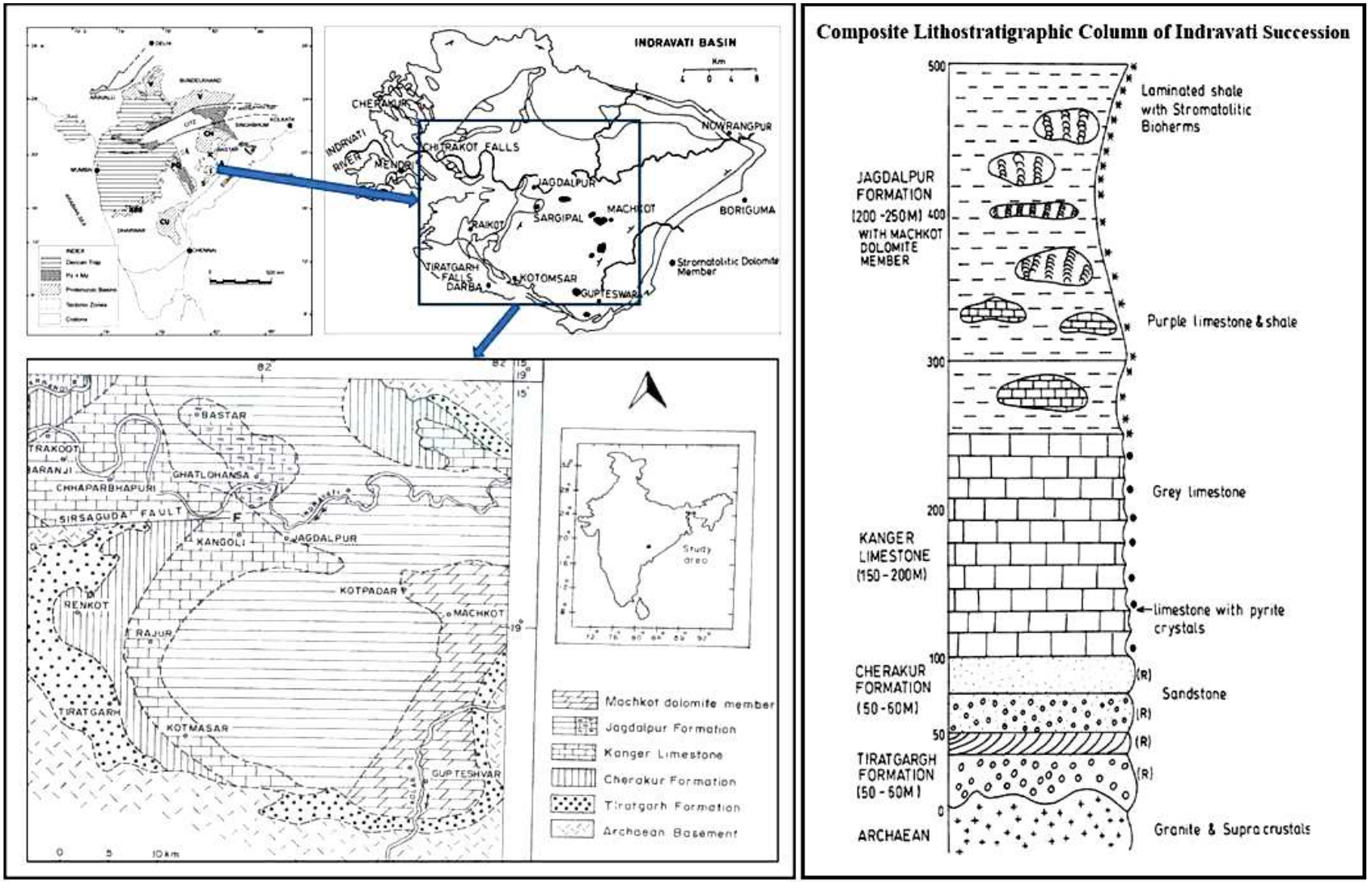

Fig. 1. Geology map and stratigraphic section of Indravati basin showing lithofacies and sampling locations.

elements that may become enriched under low-oxygen or euxinic water conditions (e.g. Brumsack, 2006; Algeo and Maynard, 2004). REE concentrations in carbonates is also used to reconstruct the chemistry of ancient seawater masses (Wright et al., 1987; Olivier and Boyet 2006; Webb and Kamber, 2000). Although REE concentration of carbonate rocks is relatively lower than that of the siliciclastic sediments, but their relative proportions are similar to those of terrigenous sediments (Balashov et al., 1964; Haskin et al., 1968, Ronov et al., 1974; Jarvis et al., 1975). Haskin et al. (1966) and McLennan et al. (1979) suggests that the carbonate phase may carry considerable portions of REE content of carbonate rocks and the incorporation of REE into carbonate minerals and the their behaviour during diagenesis was studied by Parekh et al. (1977), Scherer and Seitz (1980), and Shah and Waserburg (1985)

Therefore, the study of the trace and REE geochemistry combined with field description and the thin-section petrographic study is the appropriate means of characterizing the carbonate lithofacies. Their distribution in modern shallow seawater differs significantly from that of all known input sources. Modern and ancient carbonate rocks have been shown to record reliable marine REE signatures (Webb and Kamber, 2000). The data can also be used to test whether the Precambrian marine environment was reducing and whether terrestrial weathering was already significantly influencing marine chemistry.

GEOLOGICAL SETTING

The Indravati Group rocks unconformably overlie the Precambrian Gneissic Complex and are essentially horizontally bedded with low dips from 5 to 10 degrees. Ball (1877) and King (1881) were the earliest to describe the general geology and stratigraphy of these rocks. They have noted that these sedimentary rocks have resemblance to the Kurnool or Cuddapah Formations. The informal stratigraphic nomenclature first proposed by Crookshank (1963) was later revised by Dutt (1963), Schnitzer (1969), Krupanidhi (1970), Sharma (1975) etc. The most recent classification of lndravati basin was proposed by Ramakrishnan (1987) (Table 1). The stromatolite assemblages have been studied by Schnitzer (1971), Jairaman & Banerjee (1980), Jha et al. (1999), Guhey & Wadhwa (1993), Moitra (1999), and Guhey et al.(2011) from carbonate rocks of Indravati and Chhattisgarh Basins. These stromatolites can be correlated with upper Vindhyans and a tidal flat depositional environment (Subtidal to Intertidal) was suggested for their deposition.

Table 1. Geological succession of Indravati Basin(Ramakrishnan,1987).

	Formation	Member	Lithological Description
Indravati Group (Proterozoic)	**Jagdalpur Fm.**	Calcareous Shales with purple and gray stromatolitic dolomite (Machkot Dolomite Member)	Consists of shale, limestone and dolomite. Stromatolites are restricted to Upper part of the Jagdalpur Formation. The shale is ferruginous at places but calcareous; found with and within the Jagdalpur limestone as capping and intercalations. Limestone is hard and compact, pinkish to buff in colour, stromatolitic in nature and very well exposed.
	Kanger Limestone	Purple limestone Gray limestone	Consists of limestone. The upper part of this formation gradually becomes argillaceous in nature. The Limestone is hard and compact and breaks with conchoidal fracture and varies in colour from grayish grey to dark grey. Due to the major fault of Sirisguda, the limestone is greatly affected particularly in thickness and disposition. Burrowing structure and speleothemes are observed.
	Cherakur Fm.	Purple shale with arkosic sandstone and chert pebble conglomerate grit.	Mainly arenaceous unit consists of shales with chert pebble conglomerate, grit, arkosic sandstone and siltstone. Shales, abundant in mica (muscovite) content with prominent bedding, are used as roofing slabs.
	Tirathgarh Fm.	Chitrakoot member Mendri member	Comprises of two units (lower coarse clastic Mendri Member unit with subarkose, conglomerate, orthoquartzites and the upper fine clastic Chitrakoot Member with of sandstone/siltstones with shale interbeds. Sandstone display cross-bedding and ripple marks.
	---------- Unconformity ----------		
	Archaean		Granites and supracrustal

The sedimentary succession of the Indravati Basin, designated as Indravati Group is represented by four formations viz. Tiratgarh, Cherakur, Kanger and Jagdalpur Formations (Ramakrishnan,1987). The detailed stratigraphy and lithological characters of the Indravati succession are given in Table 1 and the general geology of the study area in Fig.1.

Following Kah et al. (2001), carbon isotope data of Indravati carbonate indicates that they appears to have been deposited during the Mesoproterozoic-Neoproterozoic transition (~1.25 to ~0.85 Ga), a period characterized by moderately positive ä13C values (~4.) (Maheswari et al., 2005). Two broad carbonate lithofacies (A & C) separated with a shale lithofacies (lithofacies B) are identified (represented by Kanger and Jagdalpur Formations) based on the field observations. The lithofacies A is represented by a well laminated/bedded black/gray pyrite bearing lime mud (belonging to Kanger limestone of Ramakrishnan, 1987), the lithofacies B represented by the purple gray calcareous shale and lithofacies C is purple gray stromatolitic dolomite belong to the Jagdalpur Formation (Table 2). Important sedimentary structures present in the study area include the depositional (bedding and stromatolites of various types), post-depositional/erosional structures (desiccation cracks, karstic features, stylolites, veinlets etc.) and the deformational (minor faults).

MATERIALS AND METHODS

In all 27 representative samples collected from various levels of the stratigraphic succession (Fig.1), which include 15 samples from Kanger Limestone (lithofacies-A), 2 samples from the calcareous shale (lithofacies-B) and 10 samples from the stromatolitic limestone (Lithofacies-C) of the Jagdalpur Formation were collected for the detailed mineralogical, petrographic and geochemical analyses.

The mineralogical composition of the various rock samples was determined by XRD and the thin sections were examined under the petrological microscope for their texture, framework composition and diagenetic modifications. The trace and rare earth element (REE) concentrations were determined by Perkin Elmer ICP-MS instrument (Elan DRC II Model) at the NGRI laboratories, Hyderabad. The JLs (Limestone) standard was used for the comparison and estimation of variation. The precisions of the elemental (trace and rare earth) data are well within accepted levels (< 6% RSD) with comparable accuracies (Balaram, 1993) of variation. The Eu and Ce were calculated following the formulae of McLennan 1989.

MINERALOGY AND PETROGRAPHY

Petrographic observation and XRD analyses of carbonate rock shows the predominantly calcite mineralogy of Lithofacies A and calcite with dolomitization confined to Lithofacies-C. The presence of chert could be indicative of late diagenetic replacement.

Different representative lithotypes of carbonate sequence of Indravati Group were identified on the basis of field and thin section petrography. The textural terminologies of Folk (1962) and Dunham (1962) have been followed in the study. Thin section petrography reveals the presence small allochem (calcareous algal filamental particles/carbonate intraclasts), micrite sized particle components. The main orthochemical constituents include the micrite, sparry calcite cement, pseudospar/neomorphic spar, replacement dolomite, pyrite etc. were present.

Various environmentally significant carbonate microfacies identified based on the detailed petrography include: i) Bedded or Laminated Micrite: occurs in Lithofacies A and consists of continuous laminae made-up of micrite alternating with a fine clastic grains are arranged parallel to laminae (Plate.1.1 & Plate.2.1). The laminated structures are produced by the construction of microbial mat through cyanobacteria. Bedded micrite contains alternate black organic layer and white crystalline layer and clear crystalline calcite layer with occasional presence of pyrite crystals, ii) Structureless micrite: occurs in lithofacies A and consist of micrite without laminations, so it's name given structureless micrite. (Plate2.2), iii) Pelmicrite: occurs in lithofacies A and contains small rounded grains of homogeneous micrite cemented by calcite and occasionally by silica (Plate.2.3), iv) Intramicrite/Intrasparite: is characteristic of lithofacies C and consists of elongated fragments of partly lithified carbonate mud. Reworking of desiccated sediments on tidal flats produces Intramicrite/ Intrasparite, and v) Dolomitized stromatoliticmicrite/ Dolospar: is representative of lithofacies C and characterized by partial fabric selective to non fabric selective replacement of stromatolitic micrite (Plate.2.4 to 2.6). In fabric selective replacement, dolomitization occurs parallel to algal lamination (Locality: Junaguda village, (Plate 1.6 & Plate.2.5)). Dolomitized rhombs represent euhedral to subhedral shape with clouded cores (Plate.2.6). The partial dolomitization gradually turns to total dolomitization towards the younger part of the succession (Locality: Gupteshwar village). Dolomite rhombs are tightly packed and forming idiotopic mosaic of euhedral dolomite and here stromatolitic structure is totally obliterated (Plate.2.6). Replacement nature of dolomite is characterized by the presence of dolomite rhombs along joints, fracture and algal laminations, clouded cores of micrite within the dolomite rhombs, progressive dolomitization obliterating the primary textures and structures and coarse crystal size of dolomite in comparison to calcite matrix. The source of Mg for extensive dolomitization in the area is supposed to be within the basin, as trapped brines in the subsurface.Dolomitization is more common to stromatolitic limestone of Jagadalpur formation and it commonly replaces micrite and shows patchy

Table 2. Summary of geochemical parameters of Indravati carbonate succession.

	Lithofacies - A				Lithofacies - B				Lithofacies - C				All Samples			
	Mz	Min	Max	σ	Mz	Min	Max	σ	Mz	Min	Max	σ	Mz	Min	Max	σ
B	16.12	12.99	19.41	1.86	18.74	16.81	20.67	2.73	17.19	12.77	22.36	2.73	16.91	12.77	22.36	2.46
Mn	292.40	65.05	472.32	117.64	335.25	213.51	456.99	172.17	206.62	126.36	296.08	61.82	247.92	65.05	472.32	101.59
Sc	0.22	0.10	0.59	0.14	0.38	0.17	0.59	0.30	0.15	0.06	0.42	0.09	0.19	0.06	0.59	0.14
V	15.57	5.39	50.61	13.41	30.44	10.48	50.40	28.22	14.63	5.63	42.29	8.60	16.15	5.39	50.61	12.24
Cr	9.87	5.12	28.68	7.01	19.11	7.40	30.83	16.57	9.95	4.19	27.94	6.13	10.60	4.19	30.83	7.34
Co	0.53	0.21	1.06	0.28	1.50	0.27	2.73	1.74	0.56	0.21	1.58	0.33	0.62	0.21	2.73	0.52
Ni	14.24	5.54	44.73	11.75	30.65	11.27	50.02	27.40	12.72	4.08	39.94	8.72	14.61	4.08	50.02	11.81
Cu	1.24	0.81	2.33	0.45	0.98	0.91	1.05	0.11	0.83	0.58	1.26	0.20	0.99	0.58	2.33	0.36
Zn	22.13	10.11	31.28	6.52	35.43	21.90	48.96	19.13	15.57	8.99	36.19	6.64	19.47	8.99	48.96	9.14
Rb	25.29	4.52	102.12	29.02	59.27	17.72	100.82	58.76	26.36	6.49	87.01	19.54	28.40	4.52	102.12	26.63
Sr	211.93	25.85	323.28	81.47	115.31	36.99	193.64	110.77	62.41	29.56	116.90	31.62	121.71	25.85	323.28	92.03
Y	12.32	8.77	23.17	4.65	16.95	9.31	24.59	10.81	8.69	2.86	19.69	4.10	10.64	2.86	24.59	5.23
Zr	304.49	75.23	1077.40	290.97	655.93	241.53	1070.34	586.06	311.28	84.28	1146.86	258.00	334.30	75.23	1146.86	294.89
Nb	64.66	15.80	223.03	61.42	126.69	57.24	196.14	98.22	58.53	16.62	218.19	49.60	65.85	15.80	223.03	57.60
Cs	2.22	0.38	9.40	2.71	5.97	1.31	10.63	6.59	2.48	0.47	11.20	2.58	2.65	0.38	11.20	2.95
Ba	283.37	1.59	657.53	301.36	502.07	449.45	554.68	74.41	129.16	48.39	386.49	83.58	213.90	1.59	657.53	218.63
Hf	8.63	2.00	31.09	8.46	19.47	7.11	31.83	17.48	9.02	2.37	33.95	7.68	9.65	2.00	33.95	8.74
Ta	0.34	0.09	1.18	0.32	0.42	0.42	0.43	0.01	0.37	0.11	0.65	0.18	0.36	0.09	1.18	0.23
Pb	1.34	0.78	2.73	0.57	1.45	1.10	1.80	0.49	1.08	0.87	1.49	0.20	1.21	0.78	2.73	0.40
Th	1.87	0.50	6.53	1.77	3.86	1.42	6.31	3.46	1.71	0.46	6.26	1.42	1.93	0.46	6.53	1.72
U	0.86	0.36	2.50	0.69	1.57	0.65	2.50	1.31	0.78	0.25	2.74	0.61	0.87	0.25	2.74	0.68
La	8.76	4.79	24.74	6.23	16.03	6.98	25.08	12.80	6.60	1.80	22.19	4.92	8.10	1.80	25.08	6.25
Ce	28.07	12.58	79.10	20.84	60.18	22.40	97.95	53.42	26.01	7.25	86.84	19.57	29.30	7.25	97.95	23.38
Pr	2.39	1.33	6.45	1.60	4.29	1.79	6.78	3.53	1.73	0.49	5.70	1.25	2.17	0.49	6.78	1.64
Nd	10.16	5.79	26.51	6.44	17.49	7.43	27.54	14.21	7.12	2.02	22.08	4.84	9.01	2.02	27.54	6.54
Sm	1.94	1.34	4.26	0.92	2.88	1.36	4.41	2.16	1.13	0.36	3.17	0.68	1.56	0.36	4.41	1.01
Eu	0.04	0.03	0.07	0.01	0.05	0.03	0.07	0.03	0.02	0.01	0.05	0.01	0.03	0.01	0.07	0.02
Gd	2.07	1.32	4.70	1.07	3.27	1.57	4.98	2.41	1.40	0.42	3.75	0.80	1.79	0.42	4.98	1.12
Tb	0.26	0.18	0.56	0.12	0.40	0.20	0.59	0.28	0.17	0.05	0.44	0.09	0.22	0.05	0.59	0.13
Dy	2.72	1.84	5.84	1.28	4.18	2.04	6.31	3.02	1.85	0.55	4.79	1.03	2.35	0.55	6.31	1.39
Ho	72.82	48.05	153.76	33.21	110.87	57.33	164.41	75.72	51.56	16.07	132.68	28.46	63.83	16.07	164.41	36.42
Er	67.53	41.64	146.28	32.49	104.17	52.22	156.12	73.47	48.83	14.56	128.20	27.59	59.86	14.56	156.12	35.02
Tm	58.16	35.10	130.70	29.11	89.52	42.31	136.73	66.77	42.31	12.62	120.47	25.98	51.68	12.62	136.73	31.70
Yb	1.54	0.96	3.53	0.79	2.45	1.17	3.74	1.82	1.08	0.31	2.99	0.65	1.35	0.31	3.74	0.85
Lu	1.48	0.92	3.42	0.77	2.30	1.08	3.53	1.73	1.00	0.26	2.88	0.63	1.28	0.26	3.53	0.82
Th_U	2.06	1.27	2.61	0.39	2.36	2.20	2.53	0.24	2.13	1.73	2.37	0.21	2.12	1.27	2.61	0.29
La_Th	5.52	3.79	9.50	1.73	4.45	3.98	4.92	0.67	4.00	2.89	4.68	0.53	4.60	2.89	9.50	1.32
SREE	259.81	156.84	596.44	136.19	421.93	199.31	644.55	314.83	192.54	57.23	542.48	117.52	234.44	57.23	644.55	147.08
Eu(an)	0.06	0.05	0.11	0.02	0.05	0.05	0.05	0.01	0.04	0.04	0.05	0.00	0.05	0.04	0.11	0.02
La/Yb	3.64	2.47	4.73	0.66	4.29	4.05	4.53	0.34	3.96	3.31	5.01	0.44	3.87	2.47	5.01	0.55
La/Lu	0.58	0.39	0.75	0.10	0.70	0.67	0.74	0.05	0.66	0.56	0.80	0.07	0.63	0.39	0.80	0.09
Ce(an)	1.53	1.25	1.76	0.17	1.82	1.66	1.99	0.23	2.00	1.88	2.28	0.10	1.81	1.25	2.28	0.26
Gdsn/Gd*	1.17	0.97	1.24	0.08	1.22	1.21	1.24	0.02	1.27	1.20	1.30	0.03	1.23	0.97	1.30	0.07
Ndsn/Ybsn	2.23	1.48	2.62	0.33	2.40	2.22	2.57	0.24	2.26	1.88	2.57	0.19	2.26	1.48	2.62	0.25
Dysn/Ybsn	1.16	0.95	1.29	0.09	1.12	1.10	1.14	0.03	1.14	1.03	1.26	0.07	1.15	0.95	1.29	0.08
Y/Ho	0.17	0.15	0.19	0.01	0.16	0.15	0.16	0.01	0.17	0.15	0.19	0.01	0.17	0.15	0.19	0.01
Pr/Pr*	0.82	0.77	0.88	0.04	0.76	0.73	0.79	0.04	0.71	0.66	0.74	0.02	0.76	0.66	0.88	0.06

an- anomaly; sn-shale normalized; Mz = Mean (Average); σ= standard d Min = Minimum; Max = Maximum

Bedded limestone, Kanger limestone, Locality: Badanjī.

Intercalation of Calcareous Shale unit within limestone. Locality: Near Kangoli

Stromatolitic limestone showing stylolite veins and karst topography,(sink holes and Natural bridge) Locality: Jagdalpur Town

Isolated Bioherm of dolomitic limestone, Jagdalpur Formation, at the basin margin,can be comparable to Modern Shark Bay, Locality Junaguda

Plate 1. Field Photographs.

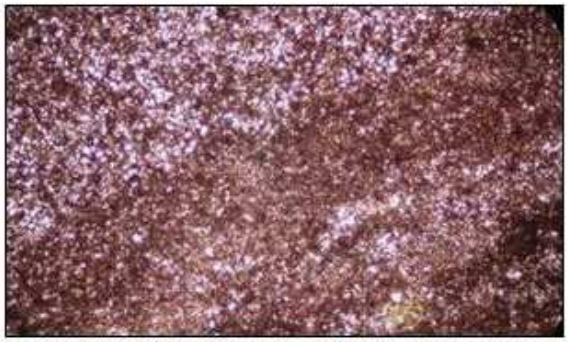

1. Laminated micrite with alternate light and dark micro-crystalline layers at upper stratigraphic horizon. Redstained grains are or calcite. Light, unstained grains correspond to dolomite & quartz.

2. Structureless micrite or massive micrite is composed of micrite without any visible structures like bedding, algal lamination etc.

3. Stained slide of Stromatolitic Micrite. Calcitic micrite is pink stained, the white is silicious.

4. Laminated algal micrite showing stylolitic boundaries. Also seen in the section a quartz filled vein.

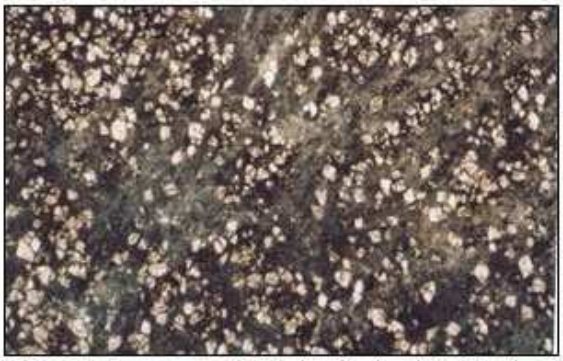

5. Microdolospar, a result fabric selective (algal laminae) dolomitization in stromatolitic dolomicrite at Loc Junaguda..

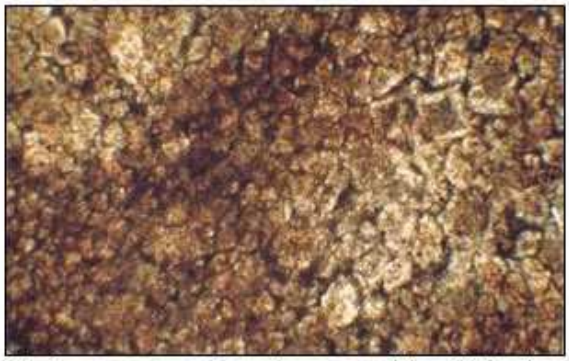

6. Dolospar representing replacement origin of dolomite resulted in formation of idiotoic mosaic of euhedral dolomite Jagdalpur Fm. Sample Loc. Gupteshwar.

Plate 2. Photomicrographs.

distribution and enhances porosity of rock. The dolomitic rhombs exhibit fabric selective (idiotopic) to pervasive (xenotopic) mosaic (Plate.2.6) that strongly suggestive of burial diagenesis. Geochemical investigations of Jagdalpur formation reveal low Sr, higher Mn content that suggest reducing condition and support burial diagenesis of dolomite. The source of Mg^{+2} for dolomitization was probably the underlying thick shale succession. It is suggested that the conversion of smectite to illite during increasing burial releases Mg^{+2} as well as Fe+2 which might be responsible for dolomitization.

GEOCHEMISTRY

Trace element data are widely considered as useful indicators of source area, tectonic setting and depositional environments (Taylor and McLennan, 1985; Bhatia,1985, Culler et all,1988; Algeo and Maynard 2004; Brumsack 2006; Maravelis and Zelilis, 2010). In the same way, REE concentrations have also been used in the reconstruction of the chemistry of ancient seawater masses during the formation of carbonates (Wright et al., 1987; Olivier and Boyet, 2006; Webb and Kamber, 2000 etc.). The trace elements in sedimentary rocks mostly reside in (a) as accessory mineral fraction, (b) adsorbed in exchangeable clay mineral sites and in clay mineral structure and (c) as organic complexes (Totten & Hanan, 1998). Non-clay minerals like quartz, feldspar in clastic rocks and contain very low concentration of trace elements. Most investigations on sedimentary carbonate rocks and minerals although reported in general a lower total REE, however, carbonate REE patterns are similar to clastic sedimentary rocks. Selected trace elements and REE analyzed for all the Indravati samples and their relative variation has been presented in Table 3. Cs, Ba, Rb, Sr, Cr, V, Sc, Ni, Ga, Co, Cu and Pb are depleted compared to PAAS for all the samples. The mean content of Ce & Y for the two carbonate units (Lithofacies A & B) is much less than that of PASS (80.00).

Strontium

Sedimentary geochemists prefer to use Sr as tool for facies analysis, while petroleum geochemists use Sr for identification of oil basins associated with carbonates. Generally Sr concentration is more in sea water than in fresh water and therefore, it reflects the nature of depositional basin water characteristics. Sr content in the present samples ranges from 25.85 to 323.28 ppm with a mean content of 211.93 ppm for Lithofacies A and 29.56 to 116.90 ppm with a mean content of 62.41 ppm for Lithofacies B (Table 3). In the present samples Sr shows a positive correlation with Mn (r = 0.521) and Cu (r = 0.398) while showing negative correlation with Ta (r= -0. 387). No correlation of Sr is observed with ∑REE.

Lead, Zinc and Nickel

The uniform presence of Pb, Zn and Ni in the present samples is interesting. Generally pelagic clays show higher concentration of Zn than near shore. The relatively lower concentration of Zn (mean ppm of 22.13 for Lithofacies-A and 15.57 for Lithofacies-B) in these rocks are related to shallow near shore phase. Nickel is very stable in aqueous solutions and capable of migration over long distance. The weathering of source rock gives rise to Fe, Ni and Si.

As the aqueous solution sinks Fe oxidizes and precipitates as ferric hydroxides, and then loses water ultimately to form goethite and hematite in which small amounts of Ni ions are trapped. In the present samples the presence of iron oxide coatings on various particles and presence of goethite (x-ray data) can be related to the consistent presence of Ni. Generally, deep see sediments show higher concentration of Ni up to 1000 ppm, whereas shallow water sediments show low concentration (Davies, 1972). The lower values of Ni (5.54 to 44.73 with a mean content of 14.24 ppm for Lithofacies-A and 4.08 to 39.94 with a mean content of 12.72ppm for Lithofacies- B) in the present samples can be related to shallow water environment of deposition.

Other Elements

The other trace elements analyzed include V, Cr, Co, Cu, Ga, Rb, Y, Zr, Nb, Cs, Ba, Hf, Ta, Th, U and REE which have been used in the interpretation of origin and provenance. The summary of the distribution of these elements and their interrelationships are shown in Tables 3 & 4. In general, the elements with low water rock coefficients and low residence time values including Zr, Hf, Ga, Y, Th, Nb, Be and REE are strongly excluded from natural waters and remain in the oceans for time less than average ocean mixing times. Consequently, it is likely that these elements are transferred quantitatively into sedimentary rocks and hence give best information regarding source rock composition. Therefore, their distribution in the sedimentary rocks is most useful for understanding the origin of the sediments. The high field strength elements (HFSE) such ZE, Y and Th are resistant to weathering compared to other trace elements (Taylor & McLennon, 1988). The present carbonate samples while showing a relatively high abundance of Zr, Y and Th display a very low concentration of Co, Sc and U. Relatively a greater variation in Ba, V and Rb is observed in Lithofacies A as compared to that of Lithofacies B. The strong positive correlation of Th with ∑REE (r= 0.967) corresponds to the relationship of REE and Th for upper crustal sediments (McLenna et al., 1980). The La/Th ratios (Fig.2) of the Indravati samples are slightly higher than those of Post-Archean or Archaean.

Table 3. Correlation coefficient matrix of Geochemical data of Indravati carbonates.

	B	Mn	Sc	V	Cr	Co	Ni	Cu	Zn	Rb	Sr	Y	Zr	Nb	Cs	Ba	Hf	Ta	Pb	Th	U	Th/U	La/Th	SREE	Eu/Eu	La/Yb	La/Lu	Ce/Ce	Gd/Gd	Nd/Yb	Dy/Yb	Y/Ho
B	1.00	-0.39	0.12	0.21	0.20	0.11	0.19	-0.13	0.16	0.20	-0.06	0.15	0.23	0.23	0.22	0.14	0.23	0.11	0.24	0.22	0.25	0.05	-0.24	0.16	-0.26	0.15	0.15	0.15	0.33	0.07	-0.10	0.01
Mn	-0.39	1.00	0.06	-0.08	-0.06	0.28	-0.01	0.10	0.27	-0.10	0.52	0.18	-0.11	-0.13	-0.07	-0.04	-0.10	-0.36	0.14	-0.08	-0.07	-0.16	0.60	0.10	0.46	-0.32	-0.37	-0.44	-0.42	-0.19	0.18	0.00
Sc	0.12	0.06	1.00	0.96	0.93	0.76	0.97	0.14	0.85	0.95	-0.16	0.96	0.94	0.95	0.93	0.62	0.94	0.65	0.41	0.96	0.95	0.52	-0.22	0.98	-0.13	0.60	0.48	0.03	0.06	0.52	-0.31	-0.74
V	0.21	-0.08	0.96	1.00	0.97	0.77	0.99	0.06	0.78	0.99	-0.34	0.90	0.98	0.97	0.97	0.59	0.98	0.69	0.35	0.98	0.97	0.55	-0.36	0.95	-0.30	0.68	0.59	0.24	0.23	0.55	-0.37	-0.73
Cr	0.20	-0.06	0.93	0.97	1.00	0.79	0.98	0.03	0.77	0.98	-0.32	0.89	0.98	0.97	0.97	0.53	0.98	0.67	0.38	0.98	0.97	0.53	-0.34	0.95	-0.27	0.64	0.55	0.26	0.20	0.47	-0.47	-0.73
Co	0.11	0.28	0.76	0.77	0.79	1.00	0.82	-0.09	0.75	0.78	-0.25	0.72	0.78	0.73	0.81	0.44	0.79	0.32	0.45	0.78	0.74	0.49	-0.21	0.77	-0.14	0.43	0.39	0.20	0.14	0.33	-0.36	-0.58
Ni	0.19	-0.01	0.97	0.99	0.98	0.82	1.00	0.05	0.83	0.99	-0.31	0.92	0.98	0.98	0.98	0.58	0.98	0.67	0.41	0.99	0.98	0.55	-0.33	0.97	-0.27	0.67	0.58	0.22	0.20	0.53	-0.40	-0.77
Cu	-0.13	0.10	0.14	0.06	0.03	-0.09	0.05	1.00	0.37	0.01	0.40	0.19	0.01	0.07	-0.01	0.36	0.01	0.09	0.35	0.04	0.07	0.00	0.10	0.13	0.12	-0.03	-0.09	-0.31	-0.14	0.12	0.14	-0.11
Zn	0.16	0.27	0.85	0.78	0.77	0.75	0.83	0.37	1.00	0.76	0.07	0.84	0.78	0.79	0.78	0.61	0.78	0.36	0.61	0.80	0.82	0.29	-0.07	0.85	-0.10	0.51	0.41	-0.03	0.04	0.51	-0.13	-0.65
Rb	0.20	-0.10	0.95	0.99	0.98	0.78	0.99	0.01	0.76	1.00	-0.39	0.90	0.99	0.98	0.98	0.55	0.99	0.72	0.36	0.99	0.97	0.58	-0.38	0.95	-0.32	0.70	0.62	0.29	0.25	0.53	-0.43	-0.76
Sr	-0.06	0.52	-0.16	-0.34	-0.32	-0.25	-0.31	0.40	0.07	-0.39	1.00	0.00	-0.34	-0.30	-0.36	0.00	-0.34	-0.39	0.10	-0.31	-0.27	-0.35	0.75	-0.13	0.80	-0.54	-0.67	-0.86	-0.75	-0.40	0.15	0.29
Y	0.15	0.18	0.96	0.90	0.89	0.72	0.92	0.19	0.84	0.90	0.00	1.00	0.89	0.90	0.88	0.55	0.89	0.56	0.46	0.91	0.92	0.44	-0.08	0.98	0.01	0.49	0.36	-0.05	-0.06	0.39	-0.37	-0.66
Zr	0.23	-0.11	0.94	0.98	0.98	0.78	0.98	0.01	0.78	0.99	-0.34	0.89	1.00	0.99	0.99	0.56	0.99	0.70	0.37	0.99	0.98	0.57	-0.38	0.95	-0.30	0.70	0.61	0.27	0.24	0.52	-0.44	-0.76
Nb	0.23	-0.13	0.95	0.97	0.97	0.73	0.98	0.07	0.79	0.98	-0.30	0.90	0.99	1.00	0.98	0.58	0.99	0.73	0.38	0.99	0.99	0.56	-0.37	0.96	-0.28	0.69	0.60	0.23	0.21	0.53	-0.44	-0.78
Cs	0.22	-0.07	0.93	0.97	0.97	0.81	0.98	-0.01	0.78	0.98	-0.36	0.88	0.99	0.98	1.00	0.51	0.99	0.63	0.35	0.99	0.98	0.50	-0.35	0.94	-0.29	0.68	0.61	0.30	0.23	0.51	-0.42	-0.75
Ba	0.14	-0.04	0.62	0.59	0.53	0.44	0.58	0.36	0.61	0.55	0.00	0.55	0.56	0.58	0.51	1.00	0.56	0.56	0.36	0.58	0.52	0.65	-0.28	0.57	-0.18	0.49	0.38	-0.07	0.13	0.51	-0.08	-0.54
Hf	0.23	-0.10	0.94	0.98	0.98	0.79	0.98	0.01	0.78	0.99	-0.34	0.89	0.99	0.99	0.99	0.56	1.00	0.70	0.36	1.00	0.98	0.57	-0.38	0.95	-0.30	0.70	0.61	0.28	0.24	0.52	-0.44	-0.77
Ta	0.11	-0.36	0.65	0.69	0.67	0.32	0.67	0.09	0.36	0.72	-0.39	0.56	0.70	0.73	0.63	0.56	0.70	1.00	0.09	0.71	0.65	0.73	-0.48	0.62	-0.40	0.61	0.54	0.27	0.34	0.42	-0.40	-0.68
Pb	0.24	0.14	0.41	0.35	0.38	0.45	0.41	0.35	0.61	0.36	0.10	0.46	0.37	0.38	0.35	0.36	0.36	0.09	1.00	0.38	0.42	0.13	-0.10	0.44	-0.01	0.14	0.08	-0.02	0.04	0.17	-0.18	-0.32
Th	0.22	-0.08	0.96	0.98	0.98	0.78	0.99	0.04	0.80	0.99	-0.31	0.91	0.99	0.99	0.99	0.58	1.00	0.71	0.38	1.00	0.99	0.56	-0.36	0.97	-0.27	0.68	0.59	0.23	0.21	0.52	-0.43	-0.76
U	0.25	-0.07	0.95	0.97	0.97	0.74	0.98	0.07	0.82	0.97	-0.27	0.92	0.98	0.99	0.98	0.52	0.98	0.65	0.42	0.99	1.00	0.47	-0.33	0.97	-0.26	0.67	0.57	0.23	0.20	0.52	-0.41	-0.75
Th/U	0.05	-0.16	0.52	0.55	0.53	0.49	0.55	0.00	0.29	0.58	-0.35	0.44	0.57	0.56	0.50	0.65	0.57	0.73	0.13	0.56	0.47	1.00	-0.59	0.50	-0.35	0.54	0.47	0.30	0.33	0.35	-0.41	-0.63
La/Th	-0.24	0.60	-0.22	-0.36	-0.34	-0.21	-0.33	0.10	-0.07	-0.38	0.75	-0.08	-0.38	-0.37	-0.35	-0.28	-0.38	-0.48	-0.10	-0.36	-0.33	-0.59	1.00	-0.18	0.74	-0.49	-0.55	-0.75	-0.73	-0.32	0.29	0.38
åREE	0.16	0.10	0.98	0.95	0.95	0.77	0.97	0.13	0.85	0.95	-0.13	0.98	0.95	0.96	0.94	0.57	0.95	0.62	0.44	0.97	0.97	0.50	-0.18	1.00	-0.11	0.58	0.47	0.08	0.04	0.47	-0.39	-0.74
Eu/Eu*	-0.26	0.46	-0.13	-0.30	-0.27	-0.14	-0.27	0.12	-0.10	-0.32	0.80	0.01	-0.30	-0.28	-0.29	-0.18	-0.30	-0.40	-0.01	-0.27	-0.26	-0.35	0.74	-0.11	1.00	-0.69	-0.76	-0.82	-0.95	-0.63	-0.15	0.32
La/Yb	0.15	-0.32	0.60	0.68	0.64	0.43	0.67	-0.03	0.51	0.70	-0.54	0.49	0.70	0.69	0.68	0.49	0.70	0.61	0.14	0.68	0.67	0.54	-0.49	0.58	-0.69	1.00	0.94	0.52	0.63	0.87	-0.02	-0.62
La/Lu	0.15	-0.37	0.48	0.59	0.55	0.39	0.58	-0.09	0.41	0.62	-0.67	0.36	0.61	0.60	0.61	0.38	0.61	0.54	0.08	0.59	0.57	0.47	-0.55	0.47	-0.76	0.94	1.00	0.63	0.68	0.81	-0.01	-0.61
Ce/Ce*	0.15	-0.44	0.03	0.24	0.26	0.20	0.22	-0.31	-0.03	0.29	-0.86	-0.05	0.27	0.23	0.30	-0.07	0.28	0.27	-0.02	0.23	0.23	0.30	-0.75	0.08	-0.82	0.52	0.63	1.00	0.77	0.33	-0.21	-0.28
(Gd/Gd*)sn	0.33	-0.42	0.06	0.23	0.20	0.14	0.20	-0.14	0.04	0.25	-0.75	-0.06	0.24	0.21	0.23	0.13	0.24	0.34	0.04	0.21	0.20	0.33	-0.73	0.04	-0.95	0.63	0.68	0.77	1.00	0.56	0.16	-0.20
(Nd/Yb)Sn	0.07	-0.19	0.52	0.55	0.47	0.33	0.53	0.12	0.51	0.53	-0.40	0.39	0.52	0.53	0.51	0.51	0.52	0.42	0.17	0.52	0.52	0.35	-0.32	0.47	-0.63	0.87	0.81	0.33	0.56	1.00	0.39	-0.51
(Dy/Yb)sn	-0.10	0.18	-0.31	-0.37	-0.47	-0.36	-0.40	0.14	-0.13	-0.43	0.15	-0.37	-0.44	-0.44	-0.42	-0.08	-0.44	-0.40	-0.18	-0.43	-0.41	-0.41	0.29	-0.39	-0.15	-0.02	-0.01	-0.21	0.16	0.39	1.00	0.30
Y/Ho	0.01	0.00	-0.74	-0.73	-0.73	-0.58	-0.77	-0.11	-0.65	-0.76	0.29	-0.66	-0.76	-0.78	-0.75	-0.54	-0.77	-0.68	-0.32	-0.76	-0.75	-0.63	0.38	-0.74	0.32	-0.62	-0.61	-0.28	-0.20	-0.51	0.30	1.00

Correlations (Indravati_Data.sta). Marked (in bold) correlations are significant at $p < .05000$; N=27 (Casewise deletion of missing data); sn-shale normalized

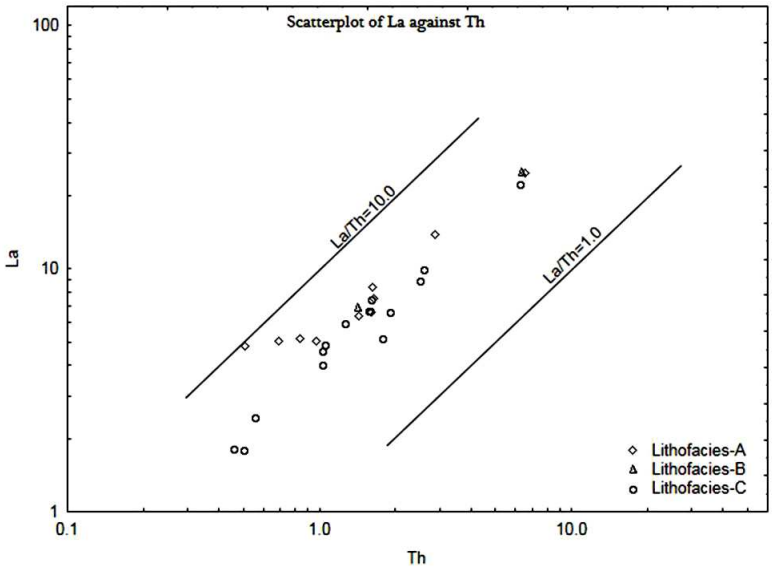

Fig. 2. Plot of La vs. Th for Indravati carbonates showing good correlation.

Rare Earth Elements (REE)

The rare earth elements (REE) are a group of 14 elements from La to Lu that exhibits generally similar chemical behaviour. Owing to their electronic configurations, these elements form ions that are nearly all trivalent, with smoothly decreasing ionic radii. Notable exceptions are stabilization of Ce^{4+} and Eu^{2+} under appropriate oxidizing and reducing conditions, respectively. Goldschmidt (1954) was first to suggest that the constant distribution of REE in sedimentary rocks is the result of homogenizing effects of sedimentary processes and therefore, the REE pattern of sedimentary rocks reflect the continental crustal abundances.

The concentration of REE is generally low in limestone than the shale, which suggest that the marine carbonate phase contains significantly lee REE than the terrigenous materials (Piper, 1974). Higher abundance of REE in clastic sediment is due to the presence of the clay fractions, because REE are readily accommodated in the clay structure (McLennan, 1989). Seawater contributes low REE to the sediments whereas the terrigenous sediment contains high REE abundance, not-similar to seawater-like pattern (Nothdurft et al., 2004).

The generally higher prevalence in nature of even atomic numbers is manifested by ratios of magnitude between neighboring pairs of elements. Consequently, comparisons among the REE are facilitated by normalizing analytical values to an appropriate reference, such as Chondrite, but for sedimentary rocks the preferred reference is either Post-Archaen Average Shale (PASS) or the North American Shale Composite (NASC), representatives of the average upper crust (Gromet et al., 1984, Condie, 1991). With respect to such a reference certain fractionation effects may enhance the light REE (LREE) or the heavy REE (HREE), and those may be quantified by the ratio of normalized $La_n/Lu_n>1$ (La/Lu>9.63) or $La_n/Lu_n<1$ respectively. Curvature in an REE plot may document an enhancement of the middle REE (MREE) with respect to both LREE and HREE. The resulting "hat-shaped" REE plat may be quantified by a ratio such as $2GD_n/(La_n/Lu_n)>1$.

REE Distribution of the Indravati Carbonate Succession

In the present study the REE have been analyzed with an objective of understanding their distribution in the carbonate lithofacies of Indravati Group, their provenance and depositional/diagenetic processes. The PAAS normalized REE patterns of sea water exhibit significant LHREE depletion, negative Ce anomaly, slight positive La anomaly (De Baar et al, 1991; Bau and Dulski, 1996) and super chondritic Y/Ho ratios (Bau, 1996). The Indravati carbonate samples show a variable REE +Y patterns resembling in some aspect to seawater pattern (ex. Significant LREE deletion) while deviating from the seawater patterns (in having a positive Ce anomaly and very low Y/Ho ratios) (Fig.3). The total concentration of REE (ΣREE) in the present sample varies from 57.23 to 644.55 with a mean content of 234.44. Both the carbonate lithofacies (Lithofacies A & C) display the total REE content of 259.81 and 192.54 ppm respectively (Table 4) which is more than the crustal average of 151.10 (after Mason and Moore, 1982). The PAAS normalized REE patterns (Fig. 4) of these rock samples are very similar to each other, (i) being significantly depleted in the LREE relative to the HREE - show a moderate degree of rare earth element fractionation when

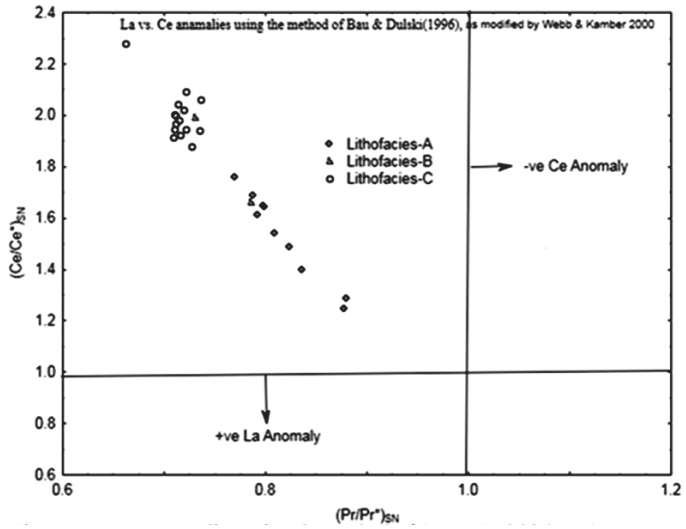

Fig. 3. La vs. Ce anomalies using the method of Bau & Dulski (1996), (modified by Webb & Kamber, 2000) differentiating the Indravati carbonates Lithofacies.

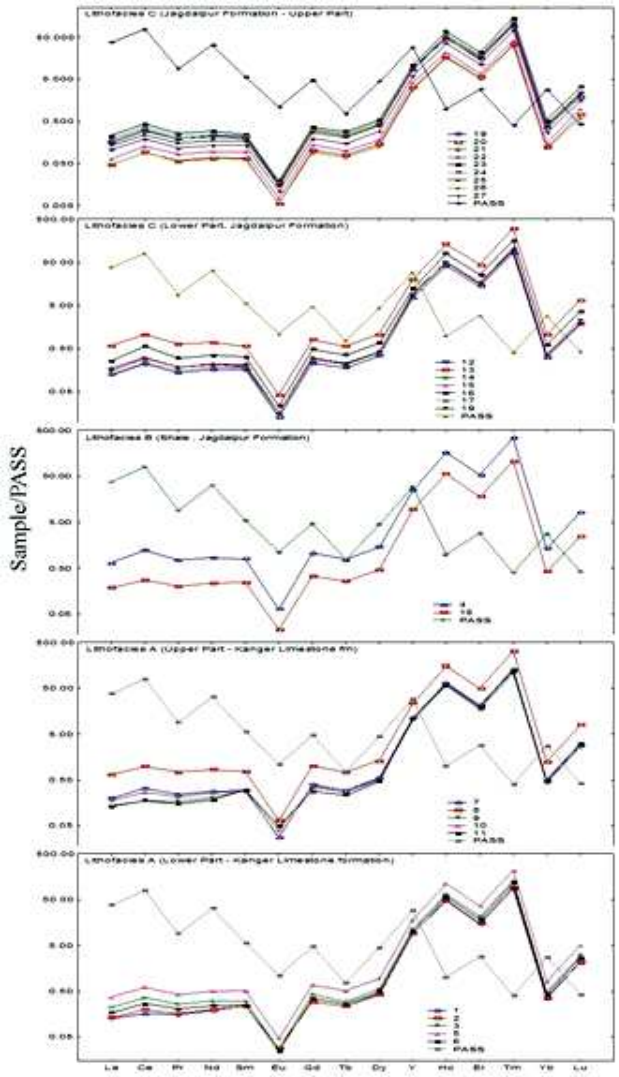

Fig. 4. PASS normalized REE+Y patterns of Indravati carbonates.

Table 4. Results of Factor Analysis of Indravati Carbonate Sequence

A. Factor Loadings (Varimax normalized)			
Variables	**Factor1**	**Factor2**	**Factor3**
B	0.1650	0.2427	-0.1741
Mn	0.0746	-0.6407	0.1678
Sc	**0.9798**	0.0106	0.0764
V	**0.9583**	0.2100	0.0092
Cr	**0.9568**	0.1925	-0.0921
Co	**0.7998**	0.0649	-0.0745
Ni	**0.9794**	0.1711	0.0005
Cu	0.1409	-0.3358	0.5467
Zn	**0.8626**	-0.1310	0.2969
Rb	**0.9586**	0.2531	-0.0476
Sr	-0.1281	**-0.9016**	0.1385
Y	**0.9642**	-0.1315	0.0050
Zr	**0.9627**	0.2354	-0.0578
Nb	**0.9675**	0.2041	-0.0268
Cs	**0.9500**	0.2315	-0.0645
Ba	0.6185	0.0347	0.4525
Hf	0.9613	0.2391	-0.0573
Ta	0.6444	0.3866	0.0097
Pb	0.4646	-0.1429	0.1094
Th	**0.9752**	0.1961	-0.0354
U	**0.9659**	0.1720	-0.0370
Th/U	0.5352	0.3808	0.0858
La/Th	-0.2102	**-0.8198**	0.0693
La/Yb	0.5824	0.6161	0.3669
La/Lu	0.4694	**0.7180**	0.3115
Y/Ho	**-0.7617**	-0.2395	-0.1505
(Eu/Eu*)sn	-0.1030	**-0.9144**	-0.2890
(Ce/Ce*)sn	0.0639	**0.9067**	-0.1290
(Gd/Gd*)sn	0.0443	**0.8866**	0.2521
(Nd/Yb)sn	0.4542	0.4549	0.6611
(Dy/Yb)sn	-0.4259	-0.0580	**0.7141**
(Pr/Pr*)sn	0.0168	**-0.9111**	0.1778
∑REE	**0.9901**	-0.0019	0.0057
∑LREE	-0.0238	0.0143	0.4516
∑HREE	**0.9870**	-0.0463	-0.0007
EigenValues	18.7382	6.0926	2.2833
Expl.Var	17.4715	7.3118	2.3307
%Total variance	49.91	20.89	6.66

B. Varimax Normalized Factor Scores			
Sample No	**Factor1**	**Factor2**	**Factor3**
1	-0.5164	-2.2293	0.8434
2	-0.3963	-1.0695	0.1608
3	-0.0533	-0.2719	2.2797
4	2.8033	-0.1520	0.1691
5	0.6897	-0.5675	0.5114
6	0.0354	-0.6155	0.7051
7	0.0548	-0.6805	2.2989
8	2.4955	0.3186	-0.2831
9	-0.3454	-1.9456	-0.4004
10	-0.0191	-0.6689	0.6146
11	-0.2713	-2.5298	-2.9292
12	-0.6654	0.5115	-0.3715
13	2.2303	0.7823	-0.5751
14	-0.3853	0.8230	-0.3170
15	-0.4103	0.7429	0.2006
16	0.2938	0.8282	-0.4880
17	-0.6327	0.3248	-0.4251
18	-0.1292	-0.1799	0.3755
19	-0.4812	0.8095	0.4927
20	-1.1630	0.9411	0.0656
21	-0.1026	0.8132	-0.6320
22	-1.0690	0.6546	0.2995
23	0.3000	0.6054	-0.5133
23	-0.2438	0.8082	0.1846
25	-0.3048	0.5140	-1.5207
26	-1.1100	0.8253	-0.3965
27	-0.6040	0.6076	-0.3495

(Marked (bold) loadings are >.700000)

sn - shale normalized

Total Variance Explained: 77.5%

compared to source rock, as indicated in their $(La/Yb)_N$ ratio of 3.64 for Lithofacies A and 3.31 for Lithofacies C samples, (ii) flat LREE and enriched HREE and (iii) a strong negative europium anomaly which is more pronounced in Lithofacies A. and (iv) a mild positive Ce anomaly. Relatively lower GD_N/Yb_N mean ratios (0.97 to 1.24; mean-1.17 for Lithofacies A and 1.20 to 1.30; mean-1.27 for Lithofacies B).

The concentration of REE in the present samples when compared to PAAS (ΣREE of PAAS) is 180; the Carbonate Lithofacies A & C show 259.81 & 192.54; the Lithofacies B (Calcareous Shale) show 421.93) is due to the presence of fine-grained clay minerals that contain high REE among the eroded materials and possibly the micrite (carbonate mud) and algal grains. Although, their REE is concentration high, the variability in terms of bulk rare earth elements and LREE/HREE ratio for all the samples is low. The change in the elemental concentration of ∑REE varying from 57.23 to 644.55 for the entire sequence as seen in the present samples (Table 3) reflect a relatively unstable tectonic conditions under which they have been evolved.

REE Anomalies

The most distinctive deviations from regular behaviour of the REE are "anomalous" levels of Ce and Eu. Understanding the origin of the depletion in Eu and Ce, relative to the other normalized REE in clastic sedimentary rocks is fundamental to most interpretations of crustal composition and evolution. A deviation of Ce and Eu may be quantified as ratio to Ce^* and Eu^* respectively by interpolating neighboring REE $\{Ce_{an} = Ce_n/[(La_n)(Nd_n)]^{1/2}$ and $Eu_{an} = Eu_n / [(Sm_n)(Gd_n)]^{1/2}\}$.

Eu Anomaly

Almost all the post-Archaen sedimentary rocks (except volcanogenic sediments) are characterized by Eu depletion (Taylor & McLennan, 1985). The negative Eu anomaly in some of these rocks indicates preferential removal of feldspar due to weathering (Nesbitt et al., 1996). The samples have a lower mean value Eu/Eu* (0.06 for Lithofacies A and 0.04 for Lithofacies B) compare to PASS/NASC representing the typical post-Archean submature sediments derived from differentiated upper continental crustal provenance (Eriksson et al., 1992). Though the rare earth elements are known to be immobile in weathering and erosion, Eu has slightly higher mobility than other REE (Albarede and Semhi, 1995).

Ce Anomaly

The possibility that Ce anomaly could be used as a possible indicator of redox conditions in natural water masses and their associated sediments, and that such sediments were preserved as reliable indicator of palaeo-redox in ancient oceans, attracted a good deal of attention in recent years (Wright et al., 1987, 88; Nothdurft et al., 2004). The Ce anomalies in marine carbonate rocks have been considered as suitable indicator of understanding the palaeo-redox conditions (Liu et al., 1988). In many past studies the palaeo-oceanographic conditions have been interpreted using the Ce behavior in the marine phases (Grandjean et al., 1987; Liu et al., 1988; German and Elderfield, 1990; Nath et al., 1997). Although. Negative Ce anomaly reveals the inclusion of REE directly from seawater or pore water under oxic-condition, the precise measurements and careful estimation of Ce anomalies in marine sediments give important aspects of the geological input and redox conditions at the time of deposition (MacLeaod and Irving, 1996). The prominent feature observed in REE distribution in present day waters and palaeo-seas is a negative Ce anomaly. If an oxic-suboxic boundary is encountered in a basin, the Ce anomaly reduces sharply to zero as Ce is re-mobilized (Sholkovitz et al. 1992). In general, strongly negative to zero Ce_{an} anomalies, and more rarely a weakly positive Ce_{an} are prominent features of REE distribution in a wide variety of modern and ancient sedimentary environments. In general the depletion of Ce relative to neighboring REE is one of the characteristic feature of seawater and marine carbonates deposited in the deep sea regions due to scavenging of Ce^{+4} by Mn oxides (Elderfield, 1988). The seawater Ce/Ce* values ranges from <0.1 to 0.4 (Elderfield and Greaves, 1982; Piepgras and Jacobson, 1992) whereas an average shale PASS/NASC Ce/Ce* is equal to 1 (Murray et al., 1991). In the present samples the value of Ce anomaly(Ce/Ce*) varies from 1.25 to 1.76 with mean value of 1.53 for lithofacies A and 1.88 to 2.28 with mean value of 2.00 for lithofacies B indicating a weakly positive Ce anomaly differing from that of the many ancient and modern sedimentary environments. The Ce/Ce* values show a negative correlation with Mn (r = -0.438) and Sr (r = -0.860) possibly suggesting the role of both redox conditions and digenesis leading to dolomitization responsible for the variation in Ce anomaly. The negative correlation between Mn and Ce/Ce* may also indicate reduction of Ce by MnO_2 (Viers and Wasserburg, 2004). The study of Takahashi et al. (2005) shows that the oxidation by Mn oxides is more plausible mechanism to produce Ce(IV)in soil horizon. The negative correlation of Ce/Ce* with Mn in the present samples could result not only from weathering process, but also by low oxygen fugacity during progressive dolomitization. The seawater signatures of the REE in the present samples are possibly masked by the abundant presence of micrite and clays and further the effect of early diagenesis and dolomitization cannot be ruled out.

STATISTICAL INTERPRETATION

The geochemical data on the Indravati Carbonate sequence has been subjected to statistical analyses for characterization of the two carbonate lithofacies. The

present study makes use of the Factor Analyses by extracting three varimax normalized factors explaining about 77.5% total variance. The results of the factor analysis are given in Table 4. The first factor explaining 49.9% total variance is display strong positive loadings of Sc, V, Cr, Co, Ni, Zn, Zr, Nb, ∑REE and ∑HREE whereas the Y/Ho ratio is the only variable showing negative relation with Factor1. The Factor1 has been related to the formation of organic complexes during the formation of the carbonates and explaining the enrichment of HREE over LREE. The Factor2, explaining 20.89% of total variance showing strong negative loadings of Sr, Eu/Eu*, Ce/Ce*, Gd/Gd* and Pr/Pr* variables and is related to the effect of diagenesis leading to depletion of LREE. The plot of factor scores of Factor1 vs. Factor2 (Fig. 5) show a clear discrimination of the lithofacies and suggesting change in the variation of depositional and diagenetic conditions of the Indravati Carbonate succession.

DISCUSSION

Shale-normalized REE+Y patterns of shallow seawater proxies have been described from both modern and ancient sedimentary environments. Suitable proxies viz. microbial carbonates, BIF, certain skeletal carbonates and pristine phosphides are primarily characterized by: (i) uniform LREE depletion; (ii) a positive La anomaly; (iii) a distinctively high Y/Ho ratios (higher than 44) and (iv) minor positive GD and Er anomalies (Alibert& McCulloch, 1993; Bau and Dulski, 1996). Further, these features are illustrated by an REE+Y pattern of average Holocene microbial carbonate that serve as a proxy for contemporary seawater owing to uniform seawater/carbonate partition coefficient (Web and Kamber, 2000). The concentration of Ce is additionally controlled by marine oxygenation levels whereas that of Eu also depends upon (i) co-precipitation with Fe-oxyhydroxides, (ii) input from high-temperature (>250°

Table 5. Lithofacies and depositional environments of Indravati carbonates.

Lithofacies and Lithology	Environment of Deposition
Lithofacies B and C Purple dolomitic shale, Pelmicrite and flat Pebble conglomerate, Purple, gray stromatolitic dolomite	**Intertidal to Supratidal**
Lithofacies A Limestone (Bedded micrite, pelmicrite etc.) Purple gray and black bedded micrite, sporadic occurrence micrites.	**Intertidal**

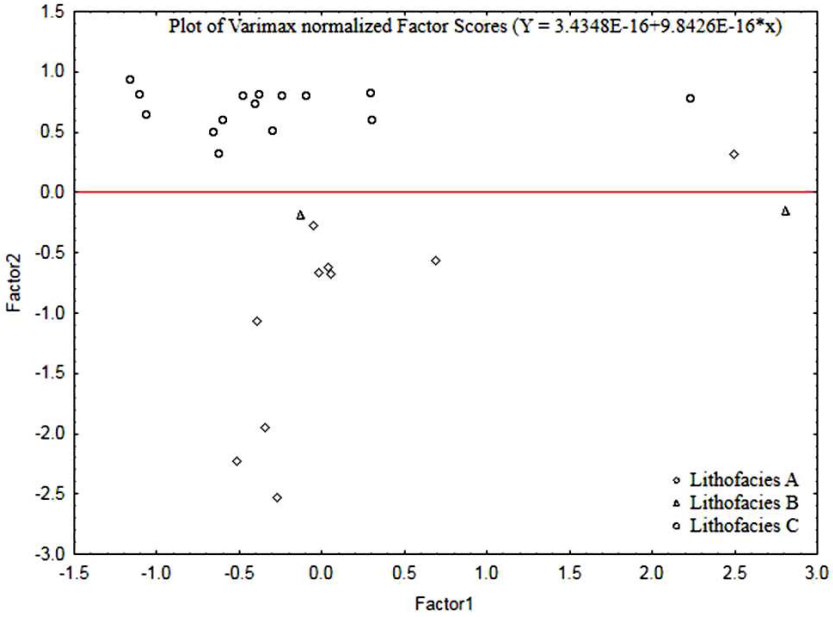

Fig. 5. Plot of Varimax normalized factor 1 vs. factor 2 differentiating the Indravati carbonates lithofacies.

C) hydrothermal sources (Michard and Albarede, 1986) and (iii) more locally the Early Archaen weathering sources that are enriched in Eu relative to post-Archaen shale (Gao and Wedepohl, 1995). However, genuine REE + Y patterns can be obscured in marine precipitates by contamination with siliciclastic or volcanic detritus, both of which contain a number of robust and different trace element signatures. Such contamination, as well as subsequent diagenetic and/or metamorphic overprinting, must be addressed before preserved patterns are interpreted.

The variations in the REE abundance patterns in Indravati carbonates are attributed to two factors: contamination with continental materials and post depositional diagenetic processes. The summary of the geochemical character of the carbonate facies is presented in Table 4. The Indravati Carbonates uniformly show REE+Y patterns characterized by LREE depletion, Lower Y/Ho ratios, positive Ce_{SN} and Er_{SN} and negative Eu anomalies (Table 3 and Fig.5). Although presence siliciclastic materials in the present samples is not observed in thin sections, due to very fine (micritic) nature of these carbonates, the LREE depletion and very low values of Y/Ho ratios and the relatively higher REE concentrations (particularly in lithofacies A & B) suggest mixing of shale. Although, the observed REE +Y patterns reflect some siliciclastic contamination but the relatively lower values of Sc and Th contradicts it. Furthermore, the samples show consistent +ve Ce, -ve Eu and +veer anomalies, all of which suggest somewhat different depositional waters unlike seawater. The chondrite/ PASS normalized REE pattern for seawater in general indicates that seawater shows a large depletion of Ce compared with the concentration of the other REE (Henderson, 1996). Ce is the only element among the mostly trivalent REEs, that can be oxidized to a tetravalent state. It is most likely removed from seawater by particulate scavenging (Buat-Menard and Chesselet, 1979) and is also fractionated into ferromanganese deposits (Glasby, 1973; Piper, 1974). In the present samples the weakly positive Ce anomaly could be due to the anoxic nature of the seawater and also low content of available Mn. The negative correlation of Mn with Ce/Ce* (r=-0.438) supports the anoxic nature of seawater.

Other features of the REE in seawater are the decreasing enrichment with increasing atomic number of the LREE, and the relatively constant, although somewhat enriched, pattern of the HREE (Table 5). The latter feature, as observed in the present carbonate samples can be explained by the formation of more stable inorganic and organic complexes by the HREE than by the LREE (Goldberg et al., 1963; Sillen and Martell, 1964).

The petrographic and XRD observations suggest the presence of calcite and dolomite in the present samples. The calcite exhibit fine grained (micrite or dolomicrite) and the dolomite crystals show a variable medium to coarse grained, anhedral to well-defined euhedral crystals (Plate.II-5 & 6). It is clear from petrography that the dolomite is of secondary origin (diagenetic replacement/recrystallization). In some samples the dolomite has been preferentially replaced by quartz, whereas the finely laminated sediments remain dolomite, suggesting that the initial sediments were more stable. The preservation of delicate lamination (Plate II-1) further supports this stable nature of carbonates. Though the original carbonates may have been calcitic or dolomitic, the diagenetic process (essentially the recrystallization and replacements) may have affected the original REE + Y pattern of the Indravti carbonates. Although, many previous studies (Tan and Hudson, 1971; Banner et., 1988; Zhong and Mucci, 1995 etc) have found that the diagenesis or early dolomitization have least effect on the REE concentrations, However, Nothdurft et al (2004) found that the dolomitization of Devonian limestones associated with basement-involved, mineralizing diagenetic fluids did alter original marine REE + Y patterns, primarily influencing on the abundance of Ce and Y content. Hence, the nature of the diagenetic fluid during dolomitization controls the degree of alteration of the REE + Y pattern. Additionally, subsequent dolomite/dolomite recrystallization may or may not alter aspects dolomite geochemistry (Land, 1992; Machel, 1997). The somewhat different REE+Y patterns (unlike the seawater) of the present samples suggest partly due to the fine non-carbonate components and the effects of the late diagenetic (burial) dolomitization which has greatly affected the REE + Y patterns and also the occurrences of various trace elements with relatively higher content of Zr, Ni, Ba and Ce. Further, the relatively higher content of Ho, Er, and Tm reported in the present study could be attributed to the presence of some silt sized heavy minerals of Zircon, Monazite? etc which also supported by higher content of Zr. Larger concentration of Ho, Er and Tm in xenotime and monazite are known to occur worldwide in many ancient and recent placer deposits, uranium ores, and weathered clay deposits (ion-adsorption ore). (http://reehandbook.com), although presence of the xenotime, monazite in the present samples is not observed due to their fine silt-size. The overall REE + Y patterns also comparable with those of Bau et al., 1996 for the Mediterranean samples differentiating the oxic v/s anoxic conditions (Fig.4f). Although, in general, the concentrations of the REE+Y in the present samples closely resembles to that of the upper crustal composition, the derivation of the framework composition of the present samples from a mixed source of origin is clearly evident from the plot of varimax normalized factor scores based on the chemical parameters wherein a clear discrimination of the two carbonate lithofacies (lithofacies A & C) is visualized. The Intervening calcareous lithofacies-B is seen separating the carbonate facies.

Depositional History of Indravati succession represented by two carbonate lithofacies (Table 5) separated by a shale lithofacies are interpreted based

on the field characteristics including the nature of the weathering surface and sedimentary structures observed suggest that deposition of the black and grey bedded micrite of lithofacies A, in tidal flat low energy environment of deposition (subtidal). While the lithofacies B consists of purple shale that gradually grading into lithofacies C that is composed of stromatolites and dolomitic micrite indicates a marine intertidal to supratidal flat environment. Desiccation cracks and mud pebbles in lithofacies C further supports their upper tidal to supratidal zone of deposition. Petrographic studies suggest that dolomitization is of secondary origin (as evidenced by stained sections showing clouded cores of dolomite crystals; larger size of dolomite crystals etc). The zonational/inclusions within the large euhedral dolomite crystals are supportive presence of Mn and Fe, that were introduced during late burial diagenesis. The some-what different REE+Y patterns, positive Ce anomaly and negative Eu anomaly and enriched HREE further supports the effect of burial diagenesis relatively at slightly higher temperatures. The significant LREE depletion compared with seawater, probably has several causes. Preponderance of basaltic REE sources in general (Condie, 1993) could have contributed this feature, but the sea water removal processes have greater potential to affect the slope of marine REE patterns. Bau and Moller (1993) and Alibert and McCullum (1993) have suggested that HREE enrichment relative to LREE could reflect higher CO2 pressure and hence different marine pH, favoring HREE stability in the water column. More efficient removal LREE in estuaries presently occurs with organic/clay complexation or carbonate complexation in estuaries where salinity increase from 2% to 10% (Hoyel et al., 1984). The persistent positive Ce anomalies in the present samples can be interpreted as a strong indication of insufficient free O to oxidize Ce to (IV) state. Under sufficiently oxidizing conditions Ce is removed very early with Fe oxides in the river water (Skolkovitz, 1992). Importantly, where such oxyhydroxide complexes were preserved as in case of Devonian estuarine carbonate sediments (Nothdurft et al, 2004), they have a positive Ce anomaly.

CONCLUSIONS

1. The carbonates comprising mainly of fine grained calcite and dolomite (fine to coarse grained) devoid of much detrital minerals display the effects of dissolution, recrystallization and replacement processes of diagenesis that is characteristic of burial diagenesis leading to dolomitization.

2. The slight variation in the PASS normalized REE+Y patterns from that of seawater are interpreted as the effect of the late stage burial diagenesis and possibly due to the minor content of non-carbonate fraction in the carbonates.

3. The HREE enrichment suggests higher CO_2 pressure and hence different marine pH (higher), and positive Ce anomaly in the carbonates are related to the oxygen deficient conditions during the deposition and/or subsequent diagenesis of the carbonates.

4. Depositional environments of Indravati carbonates can be interpreted on the basis of petrographic observation as Intertidal depositional environment for lithofacies A and Intertidal to Supratidal environment for the lithofacies B & C. The presence of desiccation cracks, various solution features and mud pebbles in lithofacies C are indicative of supratidal depositional environment and mixing of freshwater. The variation in the depositional conditions for the different lithofacies is also supported from the results factor analysis the total chemical data that clearly separate the two carbonate lithofacis and characterizes the varying depositional and diagenetic conditions of the carbonate succession.

The interpretation of each lithofacies discussed above indicates that Indravati carbonates were deposited within a broad, shallow sea marginal environment comprising of intertidal to supratidal flats.

***Acknowledgements*:** The author RG is grateful to the CGCOST for providing financial support and thankful to the Principal, Govt. NPG College of Science for extending necessary facilities. KM is thankful to the Goa University for the necessary help towards completing this work.

References

Albarede, F. (1995). Introduction to Geochemical Modeling. University Press, Cambridge, 554p.

Albarede, F and Semhi, K. (1995). Patterns of elemental transport in the bed load of the Meurthe River (NE France). Chem. Geol., 122, 129-145.

Algeo TJ, and Maynard JB (2004) Trace-element behavior and redox facies in core shale in upper Pennsylvanian Kansas-type cyclothems. Chem. Geol. 206, 289–318.

Alibert. C., and McCulloch, M. T. (1993). Rare earth element and neodymium isotopic compositions of the banded iron-formations and associated shale from Hamersley, Western Australia. Geochim. Cosmochim. Acta 57, 187-204.

Balaram, V. (1993). Characterization of trace elements in environmental samples by ICP-MS. Atomic Spectroscopy, 14(6): 174-179.

Ball, V. (1877). On the geology of the Mahanadi basin and its vicinity. Rec. Geol. Surv. India. 10(4), 167-186.

Balashov, Y. A., Ronov, A. B., Migdisov, A. A. and Turanskya, N. V. (1964). The effect of climate and

facies environment, on the fractionation of rare earths during sedimentation. Geochem. Int., 2: 951-969

Banner J. L. (1988). Rare earth element and Nd isotopic variations. in regionally extensive dolomites from the Burlington Keokuk. Formation (Mississippian): implications for REE Mobility. during carbonate diagenesis.. Jour. Sed. Petrol., 58, 415-432.

Bau, M. (1999). Scavenging of dissolved yttrium and rare earths by precipitating iron oxyhydroxide: Experimental evidence for Ce oxidation, Y-Ho fractionation, and lanthanide tetrad effect. Geochim. Cosmochim. Acta 63, 67–77.

Bau, M., Dulski, P., (1996). Distribution of yttrium and rare earth elements in the Penge and Kuruman iron formation, Transvaal Supergroup, South Africa: Precambrian Research, 79, 37-55.

Bau, M., Dulski, P. and Möller, P. (1995). Yttrium and Holmium in South Pacific Seawater: Vertical Distribution and Possible Fractionation Mechanisms. Chem. Erde. 55, 1–5.

Bau, M and Moller, P. (1993). Rare earth element systematic of the chemically precipitated component in Early Precambrian iron formations and the evolution of the terrestrial atmosphere-hydrosphere-lithosphere system. Geochim. Cosmochim. Acta, 57, 2239–2249.

Bhatia, M.R. (1983). Plate tectonics and geochemical composition of sandstones: Journal of Geology, 91, 611-627.

Brumsack H.J. (2006). The trace metal content of recent organic carbon- rich sediments: implications for Cretaceous black shale formation. PalaeogeogrPalaeoclimatolPalaoecol 232:344–361.

Buat-Menard, P. and Chesselet, R. (1979). Variable influence of the atmospheric flux on the trace metal chemistry of oceanic suspended matter. Earth Planet. Sci. Lett., 42, 399- 411.

Chatterjee N, Das N, Ganguly M and Chatterjee B (1990). Stromatolite based biostratigraphic zonation of Chandi Formation, Raipur Group, Chhattisgarh Supergroup in and around Dhamdha, Nandani area, District Durg, M.P.Geol. Surv. Ind. Spl. Publ.No. 28. 400-410.

Crookshank, H. (1963). Geology of Southern Bastar and Jeypore from the Bailadilla Range to the Eastern Ghats., Mem. Geol. Surv. India. 87, 149.

Condie, K. C. (1993). Chemical composition and evolution of the upper continental crust: contrasting results from surface samples and shales. Chemical geology, 104, 1-37.

Cullers, R.L., Barrett, T., Carlson, R. and Robinson, B., (1987). Rare earth element and mineralogic changes in Holocene soil and stream sediment: a case study in the Wet Mountains, Colorado, USA: Chemical Geology, 63(3-4), 275-297.

Davies, P. J. (1972). Trace element distribution in reef and sub reef rocks of Jurassic age in Britain and Switzerland. Jour. Sed. Petrol., 42(1), 183-194

De Baar, H.J.W., Schijf, J. and Byrne, R.H. (1991). Solution chemistry of the rare earth elements in seawater: European Journal of Solid State Inorganic Chemistry, 28, 357-373.

De Baar, H. J. W., German, C. R., Elderfield, H. and Gaans, P. V. (1988). Rare earth element distribution in the anoxic waters of Cariaco Trench. Geochim. Cosmochim. Acta, 52, 1203–1221.

Dunham, R. J. (1962). Classification of carbonate rocks according to depositional texture. In: Classification of carbonate rocks. Vol.1, (Ed. By W.E. Ham), 108-121, AAPG, Tulsa.

Dutt, N. V. B. S. (1963). Stratigraphy and Correlation of lndravati Series (Purana Group) Bastar district, M.P. Jour. Geol. Soc. India. 4, 35-49

Elderfield, H., Greaves, M.J., (1982). The rare earth elements in seawater: Nature, 296, 214-219.

Eriksson, K.A., Taylor, S.R. and Korsch, R.J. (1992). Geochemistry of 1.8-1.67 Ga mudstones and siltstones from the Mount Isa Inlier, Queensland, Australia: Provenance and tectonic implications. Geochim. Cosmochim. Acta, 56, 899-909.

Folk, R. L. (1962). Spectral sub-divisions of limestone types. In: Classification of carbonate rocks. .1, (Ed. By W.E. Ham), 62-84, AAPG, Tulsa.

Gao, S and Wedepohl, K. H. (1995). The negative Eu anomaly in Archaean sedimentary rocks-implications for decomposition, age and importance of their granitic sources. Earth and Planet. Sc. Lett., 133, 81-94.

German, C. R. and Elderfield, H. (1990) Application of the Ce anomaly as a paleoredox indicator: The ground rules. Paleoceanography 5, 823–833.

Glasby, G.B., 1973. Mechanism of enrichment of the rarer elements in marine manganese nodules. Mar. Chem., 1, 105-125.

Goldberg, E.D., Koide, M., Schmitt, R.A. and Smith, R.H., 1963. Rare earth distributions in the marine environment. J. Geophys. Res., 68, 4209—4217.

Goldschmidt, V.M., 1954. Geochemistry. Oxford University Press, Oxford, 730 pp.

Grandjean, P., Capetta, H., Michard, A and Albarede, F. (1987). The assessment of REE patterns and $^{143}Nd/^{144}Nd$ ratios in fish remains: Earth and Planet. Sc. Lett., 84, 181-196.

Guhey, R., Sinha, D., Tewari, V.C.(2011**).** Meso-Neoproterozoic Stromatolites from the Indravati and Chhattisgarh Basins, Central India. In:STROMATOLITES: Interaction of Microbes with Sediments, 21-42 (Ed. By Tewari V.C. and Seckbach, J. Springer Science + Business Media.

Guhey,R. and Wadhwa,N.P. (1993): Stromatolites from Raipur limestone around Nandini, District Durg, M.P. Ind. Jour. Earth Sci., 20 (1) 42-49.

Haskin, L. A., Haskin, M. A. and Wildeman, T. R. (1968). Relative and absolute terrestrial abundances of the rare earths. In: L.H. Ahrens(editor), Origin and sitribution of the elements. Pergamon, Oxford. 889-912.

Haskin, L.A. and Schmitt, R.A., (1976). Rare-earth distributions. In: P.H. Abelson (Editor), Researches in Geochemistry, 2. J. Wiley and Sons, New York, N.Y., 234-258.

Haskin, L. A., Wildeman, T. R., Frey. F. A., Collins, K. A., Heedy, C. R. and Haskin, M. A. (1966). Rare earths in sediments. J. Geophy. Res., 71, 6091-6105.

Holser, W. T. (1997). Evaluation of the application of rare earth elements to paleoceanography. Paleo. Paleo. Paleo. 132, 309-323.

Jairaman R.G. and Banerjee D.M. (1980). Preliminary studies of stromatolites from Raipur area, Chhattisgarh Basin, Geol. Surv. Ind. Misc. Publ. No. 44, 57-67.

Jarvis, J. C., Wildeman, T. R. and Banks, N. G. (1975). Rare earths in the Leadville Limestone and its marble derivates. Chem. Geol., 16: 27-37.

Kah, L.C., Lyons, T.W. and Chesley, J.T. (2001). Geochemistry of a 1.2 Ga carbonate-evaporite succession, northern Baffin and Bylot islands: implications for Mesoproterozoic marine evolution. Precambrian Res., 111, 203-236.

King, W. (1881). The geology of the Pranhita- Godavari Valley. Mem. Geol. Surv. India. 18 (3): 73-77.

Krupanidhi, K.V.J.R. (1970). The Purana rocks of Jagdalpurtahsil, Bastar district, M.P. Symposium on Geology and Mineral Resources of M.P. Ujjain. 3 (Abstract).

Land, L. S. (1992). The quantum theory of dolomite stabilization: does dolomite stabilize by 'Ostwald Steps'? In: Dolomite-from Process and Models to Porosity and Reservoirs, 1992 National Conference of Earth Science, Banff, Alberta, Canadian Soc. Petrol. Geologists and Faculty of Extension of University of Alberta.

Liu, X. and Byrne, R. H. (1998). Comprehensive investigation of yttrium and rare earth element complexation by carbonate ions using ICP-Mass spectrometry. J. Sol. Chem. 27, 803–815.

Liu, Y.G, Miah, M. R. U., and Schmitt, R. A. (1988). Cerium: a chemical tracer for palaeo-oceanoic redox conditions. Geochim. Cosmochim. Acta, 52: 1361-1371.

Machel, H. G. (1997). Recrystallization versus neomorphism, and the concept of 'significant recrystallization' in dolomitic research. Sed. Geolo., 113, 161-168.

Mac Leod, K.G. and Irving, A.J., (1996). Correlation of cerium anomalies with indicators of paleoenvironment: Journal of Sedimentary Research, 66, 948-955.

Maheshwari, A., Sial, A. N., Guhey, R., and Fereeira, V. P. (2005). C-isotope Composition of Carbonates from Indravati Basin, India: Implications for Regional Stratigraphic Correlation. Gondwana Research (Gondwana Newsletter Section) V. 8, No. 4, pp. 603-610.

McCulloch, M.T. and Wasserburg, G.J., (1978). Sm-Nd and Rb-Sr chronology of continental crust formation: Science, 200, 1003-1011.

McLennan, S. M. (1989). Rare earth element in sedimentary rocks: Influence of provenance and sedimentary processes. Geochemistry and Mineralogy of Rare Earth Elements, Vol. 21 (Lipin, B. R. and McKay, G A., eds.), 169–200, Mineral Society of America.

McLennan, S. M., Fryer, B. J. and Yound, G. M. (1979). The geochemistry of the carbonate-rich Espanola Formation (Huronian) with emphasis on the rare earth elements. Cam. J. Earth Sci., 16: 230-239.

McLennan, S.M., Nance, W.B. and Taylor, S.R., (1980). Rare earth element-thorium correlations in sedimentary rocks, and the composition of the continental crust. Geochim. Cosmochim. Acta, 44, 1833-1839.

Michard, A and Albarede, F. (1986). The REE content of some hydrothermal fluids. Chemical geology, 55, 51-60.

Moitra, A.K. (1999). Biostratigraphy study of stromatolites and microbiota of Chhattisgarh Basin, M.P., India, Palaeontologia Indica Geol. Surv. Ind.51, 95P.

Nath, B.N., Bau, M., Ramalingeswara Rao, B., Rao, Ch.M. (1997). Trace and rare earth elemental variation in Arabian Sea sediments through a transect across the oxygen minimum zone: Geochimica et CosmochimicaActa, 61(12), 2375-2388.

Nothdurft, L.D., Webb, G.E. and Kamber, B.S. (2004). Rare earth element geochemistry of Late Devonian reefal carbonates, Canning Basin, Western Australia: Confirmation of seawater REE proxy in ancient limestones: Geochimica et Cosmochim. Acta, 68, 263-283.

Olivier, N. and Boyet, M. (2006). Rare-earth and trace elements of microbialites in Upper Jurassic coral- and sponge-microbialite reefs. ChemiGeol 230, 105–123.

Parekh, P.P., Moller, P., Dulski, P. and Bausch, W. M. (1977). Distribution of trace elements between carbonate and non-carbonate phases of limestone. Earth Planet. Sci. Lett., 34 39-50.

Piepgras, D.J., Wasserburg, G.J. and Dasch, E.J. (1979). The isotopic composition of Nd in different ocean masses. Earth Planet. Sci. Lett. 45: 223-236.

Piper, D.Z., (1974). Rare earth elements in the sedimentary cycle: a summary. Chem. Geol, 14: 285-304.

Ramakrishnan, M. (1987). Stratigraphy, sedimentary environment and evolution of the Late Proterozoic lndravati Basin, Central India. Geo. Surv. India. 139-160.

Schere, M. and Seitz, H. (1980). Rare earth element distribution, in Holocene and Pleistocene corals and their redistribution during diagenesis. Chem. Geol., 28: 279-289.

Schnitzer, W.A.(1971). Das jungpracambrium Indiens (Purana System). Erlanger Geol.Abhi, 85, 1-44.

Schnitzer, W. A. (1969). Die Jung-algonkischen Sedimentationsraume Peninsula-Indians. N. Jb. Geol. Palaeont. Abn. 33: 191-198.

Shah, H. F. and Waserburg, G.J. (1985). Sm-Nd in marine carbonate and phosphates: Implications of Nd isotopes in seawater and crustal ages. Geochim. Cosmochim. Acta, 49: 503-518

Sharma, V. P. (1975). Note on the stratigraphic classification of the Purana rocks of Bastar district, Madhya Pradesh. Geol. Surv. India Misc. Publ. 25(1), 171-175.

Sholkovitz, E. R. (1990). Rare earth elements in marine sediments and geochemical standards. Chemical Geology, 83, 333-347.

Sholkovitz, E. R. (1992). Chemical evolution of rare earth elements: Fractionation between colloidal and solution phases of filtered river water. Earth Planet. Sci. Lett., 114, 77-84.

Sillen, L.G. and Martell, A.E., (1964). Stability constants of metal-ion complexes. Chem. Soc. London, Spec. Publ, 17: 754 pp.

Takahashi, Y., Yuita, K., Kihou, N., Shimizu, H. and Nomura, M (2005). Determination of the Ce(IV)/Ce(III) ratio by XANES in soil horizons and its comparison with the degree of Ce anomaly. Phy. Scr., 115, 936-939.

Tan, F. C and Hudson, J. D. (1971). Carbon and oxygen isotope relationships of dolomites and co-existing calcites, Great Estuarine Series(Jurassic), Scotland. Geochim. Cosmochim. Acta, 35, 755-767.

Taylor, S.R., McLennan, S. (1985). The Continental Crust: Its Composition and Evolution: Blackwell, Oxford, 312 p.

Viers, J and Waserburg, G. J. (2004). Behaviour of Sm and Nd in a laterite soil profile. Geochim. Cosmochim, Acta., 698, 2043-2054.

Walker, T. L. (1900). A geological sketch of the central portion of the JeyporeZamindari Vizagapatam district. General report for 1899- 1900. Geol. Surv. India. Mise Publ. 166-176.

Webb, G. E. and Kamber, B. S. (2000). Rare earth elements in Holocene reefalmicrobialites: A new shallow seawater proxy, Geochim Cosmochim Acta 64, 1557-1565.

Wright, J., Schrader, H., and Holser, W. T. (1987). Paleoredox variations in ancient oceans recoded by rare earth elements in fossil apatite. Geochim. Cosmochim. Acta, 51, 631-644.

Zhang, J. and Nozaki, Y. (1996). Rare earth elements and yttrium in seawater: ICP-MS determinations in the east Caroline, Coral Sea, and South Fiji basins of the western South Pacific Ocean. Geochim. Cosmochim. Acta 60, 4631-4644.

Zhang, P. S., Tao, K. J., Yang, Z. M., Yang, X. M. andSong, R. K. (2003). Rare earths, niobium and tantalum minerals in Bayan Obo ore deposit and discussion on their genesis. J Rare Earths 20(2):81–86.

Zhon, S and Mucci, A. (1995). Partitioning of rare earth elements (REEs) between calcite and seawater solutions at 25° and 1 atm, and high dissolved REE concentrations. Geochim. Cosmochim. Acta, 59, 443-453.

http://reehandbook.com.